EPJ Web of Conferences **40**, 15001 (2013)
DOI: 10.1051/epjconf/20134015001

Magnetic dynamic effects in $TbMn_{1-x}(Ga/Sc)_xO_3$ samples (x=0.4, 0.5, 0.6).

V. Cuartero[1,2], J. Blasco[2], J. García[2].

[1]ALBA Synchrotron/CELLS, 08290 Cerdanyola del Vallès, Spain
[2]Instituto de Ciencia de Materiales de Aragón, Departamento de Física de la Materia Condensada, CSIC-Universidad de Zaragoza, 50009 Zaragoza, Spain

Abstract. The magnetic properties of strongly doped $TbMnO_3$ with non-magnetic ions, such as Ga and Sc, has been studied focused in the intermediate region ($0.4 \leq x \leq 0.6$) where long range ferromagnetic ordering was reported for La-based compounds. All samples are single phase and show a perovskite structure with orthorhombic unit cell, space group *Pbnm*. The Tb-based compounds do not show long range magnetic order but magnetic anomies are noticeable at low temperature. These anomalies show magnetic irreversibility and dynamic effects typical of magnetic glassy systems. These features have been studied in detail using ac magnetic susceptibility and the analysis shows the largest magnetic correlations for x=0.5 in both type of substitutions.

1 Introduction

The occurrence of magnetic and electric long range order at the same phase is a great challenge on solid state physics. $TbMnO_3$ is a magnetoelectric multiferroic material showing these two properties at the same phase [1]. Below T_{N2}~27 K, it adopts a non-collinear magnetic arrangement which breaks the spatial inversion symmetry leading to ferroelectricity [2]. Above T_{N2}, the first magnetic transition is found at T_{N1}~41 K when Mn moments order in an incommensurate sinusoidally modulated antiferromagnetic (AFM) structure. At T_{Tb}~8K Tb sublattice also undergoes an AFM order. Moreover, the direction of the electric polarization can be switched by applying a magnetic field. So nowadays, the main challenge concerning these materials is the search of new mechanisms leading to ferroelectricity and magnetic ordering at higher temperatures, preserving the magnetoelectric coupling [3].

The dilution of the magnetic sublattice with non-magnetic ions has been successful in enhancing ferromagnetic interactions in related perovskite-like compounds such as $LaMn_{1-x}(Ga/Sc)_xO_3$. In this case, a FM ground state is found for the intermediate composition (x=0.5) [4,5]. Although the physical origin of this transition is not fully understood so far [6,7], x-ray absorption measurements confirmed that the FM ground state is concomitant with the appearance regular MnO_6 octahedra in opposite to the Jahn-teller distortion observed in $LaMnO_3$ [8].

Trying to promote ferromagnetic interactions on $TbMnO_3$, we have diluted Mn sublattice with non-magnetic ions such as Ga ($3d^{10}$) and Sc ($3d^0$). The tabulated radius of Mn and Ga are very similar (0.645 Å and 0.62 Å respectively), so the lattice modifications are expected to be very slight in this case. On the other hand, Sc^{3+} is bigger than Mn^{3+} (0.745 Å), and an increase of the unit cell has been observed for this substitution on a previous work [9]. In addition, the local structure of Mn^{3+} is not being affected by Sc^{3+} substitution, as MnO_6 octahedra remain distorted along the whole series. Beyond other aspects, this might be related to the lack of long range magnetic ordering on $TbMn_{1/2}Sc_{1/2}O_3$ on a wide temperature range up to 300 K as revealed by neutron diffraction measurements [9].

In this work we explore in detail the macroscopic magnetic properties of $TbMn_{1-x}(Ga/Sc)_xO_3$ compounds with x~0.5 in order to gain insights on the magnetic phase diagram of this diluted compounds.

2 Experimental section

The powdered samples of $TbMn_{1-x}Sc_xO_3$ were prepared by solid state reaction as reported elsewhere [9]. All samples were checked by x-ray diffraction at room temperature using a using a Rigaku D/max-B diffractometer with a rotating anode, selecting the Cu K_α wavelength (λ=1.5418 Å). They were all single phase. In the case of $TbMn_{1-x}Ga_xO_3$ the ceramic method did work only for x=0.4, while for the others two samples competitive garnet phase is also formed. Therefore, to obtain x=0.5 and 0.6 compositions we have developed a new synthesis route combining a sol-gel method and fast quench. The citrate route was used to obtain an

amorphous homogeneous starting material. After that, pellets of the precursors were heated suddenly at 1300 ºC during 5 min. and then quenched into water. The samples obtained in this way were single phase orthorhombic perovskites indicating that the formation of this phase is the fastest in this composition range (kinetic control phase). The crystallographic structure has been refined with Fullprof and the lattice parameters are detailed on table I. Ga dilution of Mn sublattice decreases the volume on the unit cell, while Sc dilution increases it, as expected.

Table I. Lattice parameters (in Å) and volume of the unit cell.

x	a	b	c	V
Ga0.4	5.2976(1)	5.7577(2)	7.4575(3)	227
Ga0.5	5.2916(4)	5.6767(4)	7.4902(6)	225
Ga0.6	5.3016(5)	5.6525(5)	7.5310(5)	226
Sc0.4	5.3771(1)	5.7412(1)	7.6922(2)	237
Sc0.5	5.3976(2)	5.7281(1)	7.7604(2)	240
Sc0.6	5.3991(2)	5.7167(3)	7.7745(3)	240

Magnetic measurements have been carried out on a commercial squid magnetometer (MPMS-5s, Quantum Design). The temperature dependence of DC magnetization has been studied between 4 K and 300 K, while we also performed hysteresis loops at 5 K and -50kOe ≤ H ≤ 50kOe. In addition, we have explored the magnetic dynamical behavior by means of ac-susceptibility measurements at low temperatures, being h_0=4 Oe and at different frequencies, ranging between 2 Hz and 1 kHz.

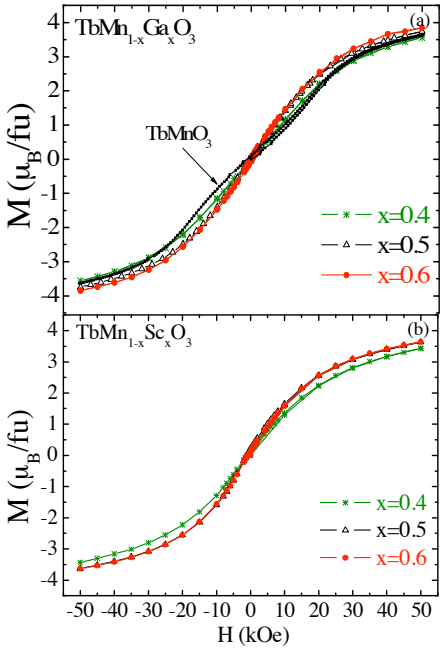

Fig. 1. Hysteresis loops at T=5K for (a) Ga-doped samples and (b) Sc-doped samples. Hysteresis loop of a $TbMnO_3$ powder sample is plotted for comparison.

3 Results and conclusions

Hysteresis loops at T=5K of all compounds are plotted on Figure 1. $TbMnO_3$ is also plotted for comparison. Both series of samples exhibit similar properties. There is not relationship between the Mn content and the magnetic moment at 50 kOe. This moment ranges between 3.4 and 3.8μ_B/fu for all samples. Moreover, the lower doped samples (x=0.4) show a lower value of the magnetization. This result confirms that the main contribution to magnetization at high fields come mainly from Tb sublattice.

On the other hand, magnetization curves are not saturated at H=50kOe and they are far from the theoretical value for a fully saturated Tb sublattice, which is 9 μ_B/fu.

Figure 2 shows dc magnetic susceptibility under zero-field and field cooled (ZFC and FC) conditions at applied fields of 100 Oe and 2500 Oe for x=0.5. Strong magnetic irreversibility is observed for both samples. The temperature range for this irreversibility decreases with increasing the external field in both cases. The Ga-doped sample shows a plateau at low temperatures and low field (100 Oe), and FC and ZFC branches separate above this point. For higher fields (2500 Oe), a peak can be appreciated on ZFC curve at around 10 K, while the branches separate at higher temperatures (Tirr=12.5 K). In the case of the Sc-doped compound, a well- defined peak is observed at low temperatures at both magnetic fields. At the same temperature, both branches separate leading to irreversibility (T_{peak}=T_{irr}).

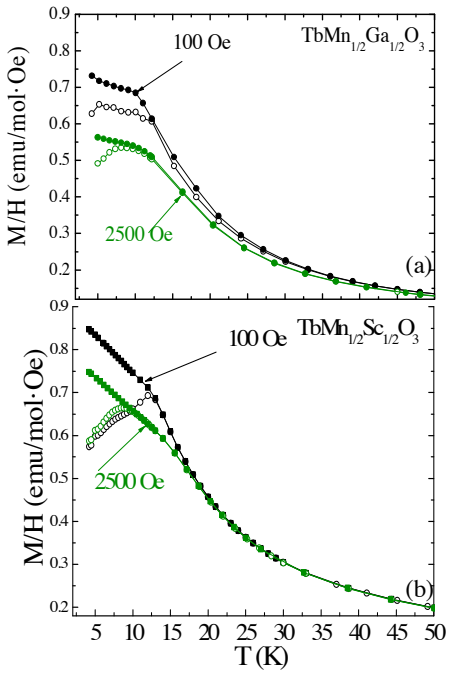

Fig. 2. Temperature dependence of Zero Field Cooled (open simbols) and Field Cooled (close symbols) curves, at H=100 Oe and 2500 Oe for (a) $TbMn_{1/2}Ga_{1/2}O_3$ and (b) $TbMn_{1/2}Sc_{1/2}O_3$.

Ac-magnetic susceptibility measurements can be observed in Figure 3 for $TbMn_{1-x}Ga_xO_3$ samples. The x=0.4 exhibits a broad maximum whose magnitude depends on the frequency of the alternating field indicating the presence of dynamic effects in this sample. The real part of χ' for the other two samples exhibits a clear peak. The peak position depends on frequency and it shifts to higher temperatures and is less intense as the frequency increases. The out of phase component χ'' also shifts to higher temperatures as frequency increases but

the magnitude of this component follows the opposite trend of the χ' component. Similar behavior can be observed in all Sc-doped samples as shown in Figure 4. These features are the hallmarks of a glassy magnetic system indicating a magnetic inhomogeneous state for all of these compounds. The presence of competitive magnetic interaction and structural disorder arising from the Mn dilution can account for the presence of magnetic glassy properties.

The factor $p=\Delta T_p/T_p \cdot \Delta(\log\omega)$ is commonly used to classify glassy magnetic systems, as it is related to the peak temperature frequency shift $T_p(\nu=\omega/2\pi)$ on the imaginary part of susceptibility, χ'' [10]. In the case of a canonical spin glass such as PdMn (RKKY interaction), p= 0.013, while on a semiconductor such as (EuSr)S or $(FeMg)Cl_2$, $p\sim$ 0.07. In all cases, the values of p range between $0.04 \leq p \leq 0.06$.

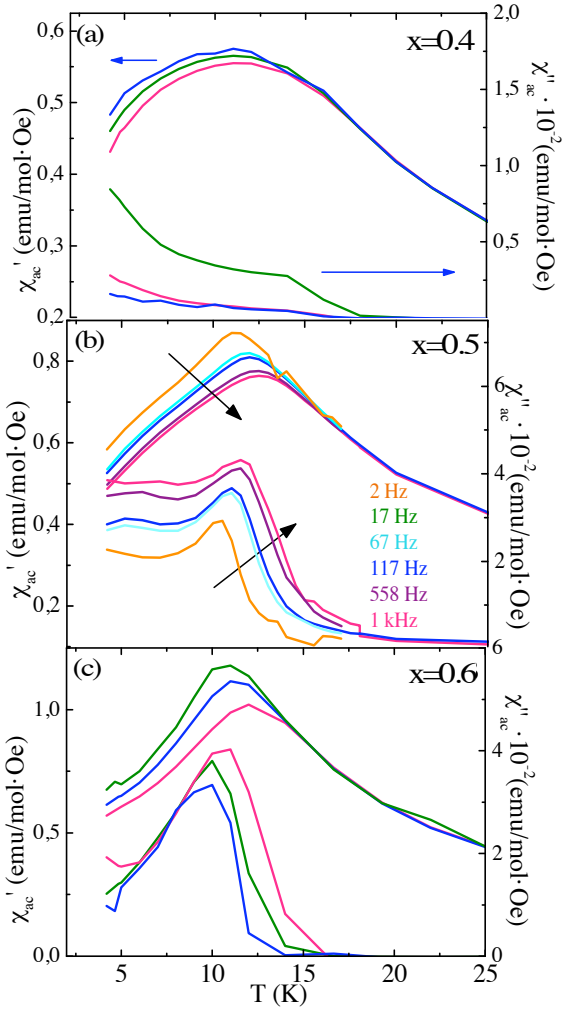

Fig. 3. Temperature dependence of ac magnetic susceptibility on $TbMn_{1-x}Ga_xO3$ series compounds at several frequencies (2 Hz, 17 Hz, 67 Hz, 117 Hz, 558 Hz and 1 kHz), being h_0=4 Oe.

Dynamic behavior in ac magnetic susceptibility can arise from thermal demagnetization process of superparamagnetic clusters and such a kind of clusters has been reported in other mixed oxides [11]. Assuming thermally activated relaxation, it is possible to describe the ac susceptibilities for independently relaxing magnetic clusters by the Néel-Arrhenius law. The Arrhenius prefactor depends on the gyromagnetic precession time and ranges between 10^{-10} and 10^{-13} seconds for superparamagnetic clusters [12]. We have fitted the frequency dependence of our xac curves to an Arrhenius law and we found unphysical small prefactors around 10^{-35} s. This result indicates that interactions exist among the relaxing magnetic entities and the magnetic transition of these samples should be described as a collective freezing.

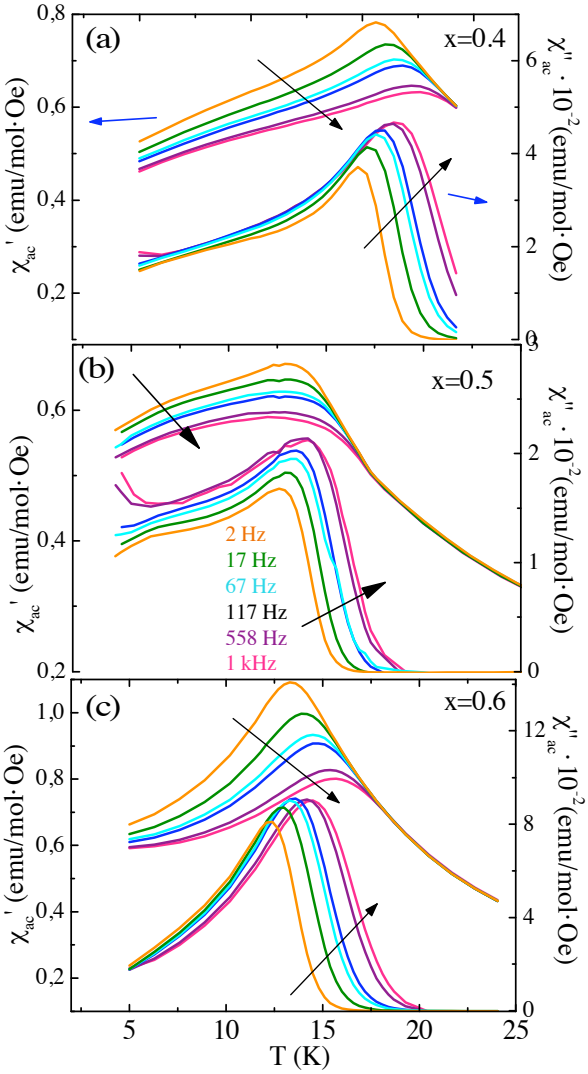

Fig. 4. Temperature dependence of ac magnetic susceptibility on $TbMn_{1-x}Sc_xO3$ series compounds at several frequencies (2 Hz, 17 Hz, 67 Hz, 117 Hz, 558 Hz and 1 kHz), being h_0=4 Oe.

Glassy magnetic systems show characteristic relaxation times ($\tau=1/\nu$) which can be fitted to Vogel-Fulcher law, that is $\tau=\tau_0\exp[E_a/k_B(T_p-T_0)]$ [13]. Here E_a corresponds to the anisotropic energy barrier and τ_0 is the characteristic relaxation time which describes the time scale of the dynamic fluctuations of the system. Typically $\tau_0 \sim 10^{-13}$ s for canonical spin glass systems, but this order of magnitude is also found in other manganites such as $Eu_{1/2}Ba_{1/2}MnO_3$ [14], where a spin glass state is observed. T_0 represents the clusters or spins interaction temperature. It is calculated from the linear relation between $(\Delta T_p(\nu)/\Delta \ln\nu)^{1/2}$ and the average temperature $\langle T_p\rangle = T_p(\nu)+\Delta T_p(\nu)/2$ [13]. The values obtained for T_0

from the dynamical scaling are shown in table II, together with the results obtained from the Vogel-Fulcher fits, shown on Figure 5 for x=0.4, 0.5 Sc-doped compounds and $TbMn_{1/2}Ga_{1/2}O_3$. The lack of a clear peak in the curve for $TbMn_{0.6}Ga_{0.4}O_3$ makes this analysis imprecise for this sample. The value of T_0 is very similar for the intermediate compounds x=0.4 and 0.5 but it starts decreasing as the non-magnetic ions concentration increases (x=0.6). The values for the anisotropic energy barrier correspond to the order of magnitude found in other cluster interacting systems [15]. The relaxation time accounting for the dynamical processes is similar for $TbMn_{0.6}Sc_{0.4}O_3$ and x=0.6 compounds. In all cases its value is a little bit larger than the relaxation time expected for an atomic scale spin-glass state. It can only be ascribed to nanosized interacting entities [16]. The shorter relaxation time is found for the $TbMn_{1/2}Sc_{1/2}O_3$ sample, being $\tau_0 \sim 10^{-8}$ s. This order of magnitude for dynamical processes is expected for a superspin or cluster glass system. Similar results are found in the Ga system. The x=0.5 composition shows the highest relaxation time and this may be related with the largest sizes of the magnetic clusters. This result might be related with an enhancement of FM interactions for x=0.5 as observed in the related La-based series [4,5].

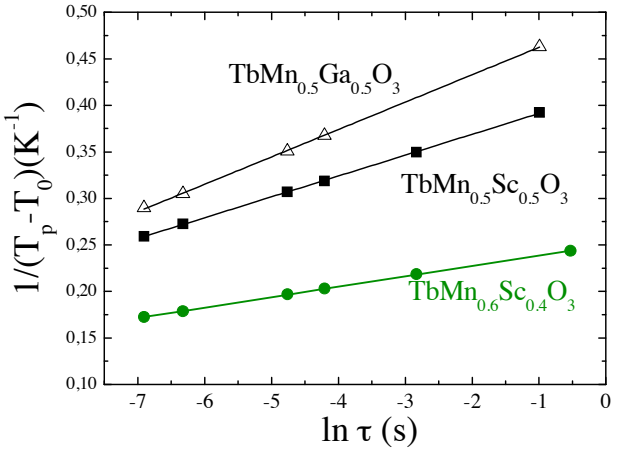

Fig. 5. Fits from the Vogel-Fulcher law for x=0.5 doped compounds and $TbMn_{0.6}Sc_{0.4}O_3$ sample.

In conclusion, the substitution of Mn with either Ga or Sc in $TbMnO_3$ does not favor the formation of a FM ground state for x=0.5 in opposite to the results observed for $LaMnO_3$. Instead, inhomogeneous magnetic samples are formed in the Tb-based series. This implies the existence magnetic frustration in these samples. This frustration arises from disorder and competitive magnetic interactions [10]. The Mn dilution easily produces structural disorder and competitive interactions may come from the strong orthorhombic distortion induced by the small size of Tb^{3+} cations [17]. In this way, the Mn-O-Mn bending weakens the superexchange FM interactions between nearest-neighbours and strengthens the antiferromagnetic interactions between next-nearest-neighbours as occurs in related $RMnO_3$ system [17,18].

The competition between FM and AFM interactions together with the random distribution of magnetic Mn^{3+} cations favours magnetic disorder but the dynamic effects observed in the ac-magnetic susceptibility suggest that x=0.5 compositions enhances magnetic correlation resulting in larger magnetic clusters.

This work was supported by MICINN (project, FIS08-03951, MAT2007-61621) and DGA (CAMRADS).

Table II. Parameters obtained from the fit to a Vogel-Fulcher law of ac-susceptibility data for x=0.5 and 0.6 Ga-doped compounds and all Sc samples.

x	T_0(K)	τ_0(s)	E_a/k_B(K)
Ga0.5	9.2	$5.6 \cdot 10^{-8}$	34
Ga0.6	5.1	$1.5 \cdot 10^{-11}$	98
Sc0.4	10.7	$2.0 \cdot 10^{-10}$	90
Sc0.5	10.1	$1.1 \cdot 10^{-8}$	45
Sc0.6	7.27	$3.6 \cdot 10^{-10}$	106

References

1. T. Kimura, T. Goto, H. Shintani, K. Ishizka, T. Arima, Y. Tokura. Nature (London) **426**, 55 (2003)
2. M. Kenzelmann, A. B. Harris, S. Jonas, C. Broholm, J. Schefer, S. B. Kim, C. L. Zhang, S.-W. Cheong, O. P. Vajk, J. W. Lynn. Phys. Rev. Lett. **95**, 087206 (2005)
3. D. Khomskii, Bull. Am. Phys. Soc. C **21** 2 (2001)
4. J. Blasco, J. García, J. Campo, M. C. Sánchez, G. Subías. Phys. Rev. B **66**, 174431 (2002)
5. J. B. Goodenough R. I. Dass, J. Zhou. Sol. State Sci.**4**, 297 (2002).
6. J. Farrell and G. A. Gehring, New J. Phys. 6, 168 (2004).
7. Y. S. Zhou and J. B. Goodenough, Phys. Rev. B **77**, 172409 (2008).
8. M. C. Sánchez, G. Subías, J. García and J. Blasco. Phys. Rev. B **69**, 184415 (2004).
9. V. Cuartero, J. Blasco, J. García, G. Subías, C. Ritter and J. A. Rodríguez-Velamazán. Phys. Rev. B **81**, 224117 (2010)
10. J. A. Mydosh, Spin glasses. An experimental introduction. Taylor and Francis, (1993).
11. S. Giri, M. Patra and S. Majumdar. J. Phys.:Condens. Matter **23**, 073201 (2011).
12. S. M. Yusuf M. Sahana, K. Dörr, U. K. Rößler, and K. -H. Müller, Phys. Rev. B **66**, 064414 (2002).
13. J. L. Tholence, Solid State Commun. **88** (1993) 917.
14. R. Mathieu and Y. Tokura. J. Phys. Soc. Jpn., **73** No. 12 124706 (2007).
15. N. Marcano, J. C. Gómez-Sal, J. I. Espeso, L.Fernández Barquín, and C. Paulsen. Phys. Rev. B **76**, 224419 (2007).
16. M. D. Mukadam,S. M. Yusuf, P. Sharma, S.K. Kulshreshtha and G. K. Dey. Phys. Rev. B **72** 174408 (2005).
17. J. Blasco, V. Cuartero, J. García and J. A. Rodríguez-Velamazán. J. Phys.: Cond. Matt. **24** 076006 (2012).
18. T. Kimura, S. Ishihara, H. Shintani, T. Arima, K. T. Takahashi, K. Ishizaka, and Y. Tokura. Phys. Rev. B **68**, 060403(R) (2003).